

Wormholes Immersed in Rotating Matter

Christian Hoffmann^{1,2,*} Theodora Ioannidou^{3,†} Sarah
Kahlen^{1,‡} Burkhard Kleihaus^{1,§} and Jutta Kunz^{1,¶}

¹ *Institut für Physik, Universität Oldenburg, Postfach 2503, D-26111 Oldenburg, Germany*

² *Department of Mathematics and Statistics, University of Massachusetts, Amherst, Massachusetts, 01003-4525, USA*

³ *Department of Mathematics, Physics and Computational Sciences, Faculty of Engineering,
Aristotle University of Thessaloniki Thessaloniki, 54124, Greece*

(Dated: June 16, 2021)

We demonstrate that rotating matter sets the throat of an Ellis wormhole into rotation, allowing for wormholes which possess full reflection symmetry with respect to the two asymptotically flat spacetime regions. We analyze the properties of this new type of rotating wormholes and show that the wormhole geometry can change from a single throat to a double throat configuration. We further discuss the ergoregions and the lightning structure of these wormholes.

PACS numbers: 04.20.Jb, 04.40.-b

I. INTRODUCTION

In General Relativity the Ellis wormhole [1–10] connects two asymptotically flat spacetime regions by a throat. The non-trivial topology is provided by the presence of a phantom field, a real scalar field with a reversed sign in front of its kinetic term. Recently, the static Ellis wormhole has been generalized to spacetimes with higher dimensions [11, 12]. Moreover, rotating generalizations of the Ellis wormhole in four and five dimensions have been found [12–15].

Since wormholes could be of potential relevance in astrophysics, a number of both theoretical and observational studies have been performed. These include astrophysical searches for wormholes [16–18], studies of their properties as gravitational lenses [19–21], studies of their shadows [22, 23] or of the iron line profiles of thin accretion disks surrounding them [24].

An Ellis wormhole carries no further fields besides the phantom field. Here we are interested in the effect of matter fields on the wormhole. To this end, we immerse the wormhole throat inside a lump of matter. While this question has been considered before for nuclear matter [25–27] and bosonic matter [28–30], the matter considered so far was non-rotating.

We here add a new twist to this quest by immersing the wormhole throat inside rotating matter, which we take as composed of a complex boson field, since this allows for the possibility to impose rotation on the bosonic field by the choice of an appropriate ansatz. The rotation of the matter then implies a rotation of the spacetime, thus dragging the wormhole throat along.

As we will see, such a rotating wormhole spacetime can be fundamentally different from a rotating wormhole without matter (except for the phantom field). Namely, the rotating configuration can be fully symmetric with respect to a reflection of the radial coordinate at its throat or in the case of a double throat at its equator. This does not hold for the rotating wormholes obtained previously [12–15], where the rotation is enforced via a boundary condition in only one of the two asymptotically flat regions.

In section II we discuss the theoretical setting to obtain wormholes immersed in rotating bosonic matter in four spacetime dimensions. Besides presenting the action, this includes a discussion of the field equations, the boundary conditions and the wormhole properties. In section III we present the results of the numerical calculations for this new class of rotating wormholes and discuss their global charges, their geometric properties, and their lightnings. We conclude in section IV.

* *Email: christian.hoffmann@uni-oldenburg.de*

† *Email: ti3@auth.gr*

‡ *Email: sarah.kahlen@uni-oldenburg.de*

§ *Email: b.kleihaus@uni-oldenburg.de*

¶ *Email: jutta.kunz@uni-oldenburg.de*

II. THEORETICAL SETTING

We consider General Relativity with a minimally coupled complex scalar field Φ and a phantom field Ψ in four spacetime dimensions. Besides the Einstein-Hilbert action with curvature scalar \mathcal{R} and coupling constant $\kappa = 8\pi G$, the action

$$S = \int \left[\frac{1}{2\kappa} \mathcal{R} + \mathcal{L}_M \right] \sqrt{-g} d^4x \quad (1)$$

contains the matter Lagrangian \mathcal{L}_M

$$\mathcal{L}_M = \frac{1}{2} \partial_\mu \Psi \partial^\mu \Psi - \frac{1}{2} g^{\mu\nu} (\partial_\mu \Phi^* \partial_\nu \Phi + \partial_\nu \Phi^* \partial_\mu \Phi) - m_b^2 |\Phi|^2 \quad (2)$$

where the kinetic term of the massless phantom field Ψ carries the reverse sign as compared to the kinetic term of the complex scalar field Φ , which possesses mass m_b .

Variation of the action with respect to the metric leads to the Einstein equations

$$G_{\mu\nu} = \mathcal{R}_{\mu\nu} - \frac{1}{2} g_{\mu\nu} \mathcal{R} = \kappa T_{\mu\nu} \quad (3)$$

with stress-energy tensor

$$T_{\mu\nu} = g_{\mu\nu} \mathcal{L}_M - 2 \frac{\partial \mathcal{L}_M}{\partial g^{\mu\nu}}, \quad (4)$$

while variation with respect to the scalar fields yields for the phantom field the equation

$$\nabla^\mu \nabla_\mu \Psi = 0 \quad (5)$$

and for the complex scalar field

$$\nabla^\mu \nabla_\mu \Phi = m_b^2 \Phi. \quad (6)$$

To allow for the non-trivial topology of the stationary spacetime, we choose for the line element

$$ds^2 = -e^f dt^2 + e^{g-f} [e^b (d\eta^2 + h d\theta^2) + h \sin^2 \theta (d\varphi - \omega dt)^2], \quad (7)$$

where f , g , b and ω are functions of the radial coordinate η and the polar angle θ , while $h = \eta^2 + \eta_0^2$ is an auxiliary function containing the throat parameter η_0 . The coordinate η then takes positive and negative values, i.e. $-\infty < \eta < \infty$, where the two limits $\eta \rightarrow \pm\infty$ correspond to two distinct asymptotically flat regions.

We parametrize the complex scalar field Φ via [31]

$$\Phi(t, \eta, \theta, \varphi) = \phi(\eta, \theta) e^{i\omega_s t + i n \varphi}, \quad (8)$$

where $\phi(\eta, \theta)$ is a real function, ω_s denotes the boson frequency, and the integer n is the rotational quantum number, which we employ to impose rotation on the field configuration ($n \neq 0$). The phantom field Ψ depends only on the coordinates η and θ ,

$$\Psi(t, \eta, \theta, \varphi) = \psi(\eta, \theta). \quad (9)$$

Substituting the above Ansätze into the Einstein equations and the matter field equations leads to a set of six coupled partial differential equations (PDEs) of second order for the unknown metric and matter functions. Inspection of this system of PDEs shows that it allows for reflection symmetric solutions with respect to $\eta \rightarrow -\eta$.

To solve this system of PDEs, we have to impose an appropriate set of boundary conditions at the boundaries of the domain of integration. For the new class of reflection symmetric rotating wormholes, which are asymptotically flat and globally regular, we impose the following conditions: (i) the metric and scalar field functions f, g, b, ω, ϕ vanish asymptotically for $\eta \rightarrow \pm\infty$, (ii) the derivatives $\partial_\theta f, \partial_\theta g, \partial_\theta \omega$ and the functions b, ϕ vanish along the rotation axis, $\theta = 0$, (iii) the derivatives $\partial_\theta f, \partial_\theta g, \partial_\theta b, \partial_\theta \omega, \partial_\theta \phi$ vanish in the equatorial plane, $\theta = \frac{\pi}{2}$.

For the phantom field the boundary conditions are more involved. While regularity and reflection symmetry with respect to the equatorial plane also require the derivative $\partial_\theta \Psi(\eta, \theta)$ to vanish at $\theta = 0$ and $\theta = \frac{\pi}{2}$, the boundary condition for Ψ can be chosen freely at one asymptotically flat boundary, since only derivatives of the phantom

field enter the PDEs, and is determined from the asymptotic form of the solutions at the other asymptotically flat boundary.

Once the solutions are obtained we can read off their physical properties. Mass and angular momentum can be obtained from the asymptotic behaviour of the metric functions

$$f \longrightarrow \mp \frac{2M_{\pm}}{\eta}, \quad \omega \longrightarrow \frac{2J_{\pm}}{\eta^3} \quad \text{as } \eta \rightarrow \pm\infty. \quad (10)$$

The particle number Q associated with the conserved current of the complex scalar field is related to the angular momentum by [31]

$$J = nQ.$$

Of interest are also the geometrical properties of the solutions. In order to determine the presence of throats and equators we consider the circumferential radius in the equatorial plane,

$$R_e(\eta) = \sqrt{h} e^{\frac{q-f}{2}} \Big|_{\theta=\pi/2}. \quad (11)$$

The minima of R_e correspond to throats, whereas the local maxima correspond to equators. Since R_e increases without bound in the asymptotic regions, any equator resides between two throats. The ergoregion of the solutions is defined as the region where the time-time component of the metric is positive, $g_{tt} > 0$. Its boundary is referred to as the ergosurface. Here $g_{tt}(\eta, \theta) = 0$.

The geodesic motion of massless particles in the equatorial plane is determined from

$$\dot{\eta}^2 = \frac{L^2}{e^{(b-q)}} \left(\frac{E}{L} - V_+(\eta) \right) \left(\frac{E}{L} - V_-(\eta) \right), \quad (12)$$

$$\text{with } V_{\pm}(\eta) = \left(\omega \mp \frac{e^{f-q/2}}{\sqrt{h}} \right), \quad (13)$$

where the derivative is with respect to some affine parameter. For circular orbits $\dot{\eta}$ and $\frac{d\dot{\eta}}{d\eta}$ have to vanish. Thus the extrema of the potentials $V_{\pm}(\eta)$ determine the location of the lightring, η_r , and the ratio $\frac{E}{L}$, i.e. $\frac{E}{L} = V_{\pm}(\eta_r)$.

III. SYMMETRIC ROTATING WORMHOLE SOLUTIONS

We have solved the above set of PDEs numerically, subject to the above boundary conditions, employing the package FIDISOL [32], a finite difference solver based on the Newton-Raphson method. The problem has the following input parameters: i) the boson frequency ω_s is varied in the interval $0 < \omega_s < m_b$ (note, that the boson mass is kept fixed throughout, $m_b = 1.1$), ii) the throat parameter is mostly fixed to $\eta_0 = 1$, though other values have also been employed (note, that $\eta_0 = 0$ leads to topologically trivial boson stars, where $\eta \geq 0$), iii) for the rotational quantum number the lowest values are considered, $n \in \{0, 1, 2\}$, where $n = 0$ represents the non-rotating case. In the following we present results for $0.3 \leq \omega_s \leq 1.03$, since for values of ω_s outside this interval the numerical errors are too large to be considered as reliable solutions (in the rotating case).

Let us start our discussion of this new type of rotating wormhole solutions by considering their global charges. In Fig.1 we show the mass M and the particle number Q versus the boson frequency ω_s for two families of rotating wormhole solutions, specified by the lowest non-trivial rotational quantum numbers $n = 1$ and $n = 2$ and the throat parameter $\eta_0 = 1$. The angular momentum J of these solutions is given by $J = nQ$. For comparison the figure also contains the corresponding set of non-rotating wormhole solutions (obtained for the same parameters except for $n = 0$) immersed in bosonic matter (see e.g. [29]).

The domain of existence of these solutions is limited by a maximal value for the boson frequency ω_s , which is reached for $\omega_{\max} = m_b$, where the family of solutions reaches a vacuum configuration with $M = 0 = Q$. This is completely analogous to the case of boson stars (see e.g. [33–38]). As seen in the figure, for large values of the frequency, the global charges of the wormholes are similar to those of boson stars, which are also exhibited with thin black lines. However the well-known spiralling behaviour of boson stars is largely lost. Instead the would-be spirals unwind after their first backbending with respect to the frequency and then continue to lower frequencies (possibly all the way to $\omega_s = 0$, where a singular configuration should be reached [29]). This unwinding is present in the case of rotating and non-rotating solutions [29, 30], and it has been seen as well in other systems with negative energy densities [39].

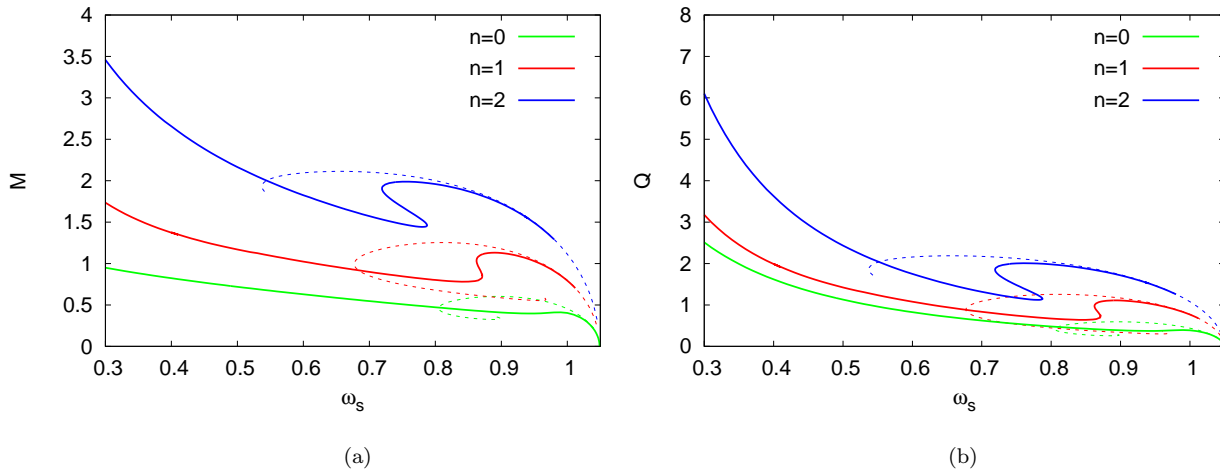


Figure 1: Global charges of symmetric wormhole solutions with throat parameter $\eta_0 = 1$ immersed in non-rotating ($n = 0$) and rotating ($n = 1, 2$) matter versus the boson frequency ω_s : (a) the mass M ; (b) the particle number Q . These configurations possess angular momentum $J = nQ$. The dashed lines indicate the corresponding boson star solutions.

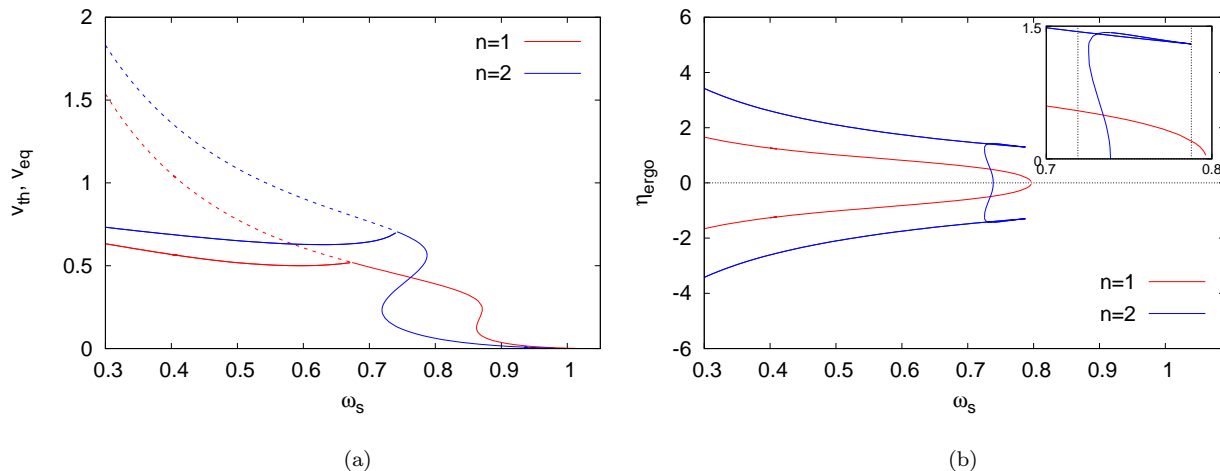


Figure 2: Throat(s), equator and ergosphere(s) of symmetric wormhole solutions with throat parameter $\eta_0 = 1$ immersed in rotating matter versus the boson frequency ω_s : (a) the rotational velocity v_{th} of the throat(s) (solid) and the rotational velocity v_{eq} of the equator (dashed); (b) the coordinate η_{ergo} of the ergosurface(s) in the equatorial plane.

Recall that we have imposed the same boundary conditions in both asymptotic regions for the metric and the complex scalar field. Thus we have not imposed rotation via the boundary conditions. Instead, the ansatz for the complex scalar field with a non-vanishing rotational quantum number n imposes rotation on the configuration.

The rotation of the scalar field implies rotation of the spacetime and consequently also rotation of the throat of the wormholes. This rotation of the throat is demonstrated for the above sets of rotating wormholes in Fig. 2(a), where the rotational velocity v_{th} of the throat(s) in the equatorial plane is shown versus the boson frequency ω_s . Also shown is the rotational velocity v_{eq} of the equator when present.

We now turn to the ergoregions of the solutions. In Fig.2(b) we show the coordinate η_{ergo} of the boundary of the ergoregions in the equatorial plane versus the boson frequency ω_s . We note that ergoregions exist only if the boson frequency ω_s is smaller than some maximal value, which depends on η_0 and the rotational quantum number n . For $n = 1$ the ergoregion decreases monotonically with increasing ω_s and degenerates to a circle residing at $\eta_{\text{ergo}} = 0$, when the maximal value of ω_s is approached.

For $n = 2$ the ergoregion decreases monotonically with increasing ω_s also up to a maximal frequency. But since this maximal frequency occurs in the range of the frequencies of the unwinding spiral, the presence of several branches of solutions complicates the picture. Following the second branch (towards smaller ω_s), η_{ergo} reaches a maximum and then decreases again. The ergoregion then disappears on the second branch before the third branch is reached.

Interestingly, for the small interval $0.7256 \leq \omega_s \leq 0.7388$ the surface of the ergoregion consists of two disconnected parts. At $\omega_s = 0.7388$, the throat at $\eta = 0$ forms an inner boundary ring, dividing the ergoregion into two parts, until at $\omega_s = 0.7256$ the ergoregion degenerates to two rings. No ergoregion exists for smaller frequencies on the second branch of solutions.

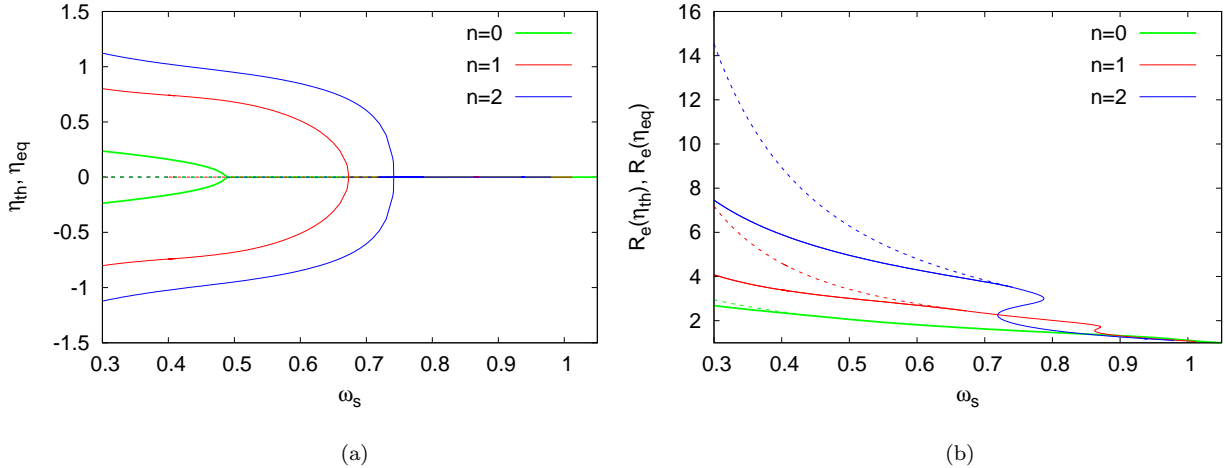


Figure 3: Throat(s) and equator of symmetric wormhole solutions with throat parameter $\eta_0 = 1$ immersed in non-rotating ($n = 0$) and rotating ($n = 1, 2$) matter versus the boson frequency ω_s : (a) the coordinate η_{th} of the throat(s) (solid) resp. the coordinate η_{eq} of the equator (dashed) in the equatorial plane; (b) the circumferential radius $R_e(\eta_{\text{th}})$ of the throat(s) (solid) resp. the circumferential radius $R_e(\eta_{\text{eq}})$ of the equator (dashed) in the equatorial plane.

Let us next consider the geometry of the wormhole solutions. In Fig.3 we present the coordinate η_{th} of the throat(s) resp. the coordinate η_{eq} of the equator in the equatorial plane as well as the corresponding values of the circumferential radius R_e . We observe that for large values of the boson frequency ω_s the wormholes possess only a single throat. At a critical value of ω_s an equator emerges, when the throat degenerates to an inflection point at the critical value of ω_s . For smaller ω_s the circumferential radius R_e possesses a maximum at $\eta = 0$, corresponding to an equator, and two minima located symmetrically at around $\eta = 0$, corresponding to two throats.

In order to get a deeper insight into the geometry of the wormholes, we exhibit in Fig.4 the isometric embedding of the equatorial plane for symmetric wormhole solutions immersed in non-rotating ($n = 0$) and rotating ($n = 1, 2$) matter with $\eta_0 = 1$ and $\omega_s = 0.3$ as examples of double-throat wormholes. Note the pseudo-euclidean embedding for the case $n = 2$.

Finally we would like to address the lightrings of these spacetimes. In Fig.5 we therefore exhibit the coordinate η_{lr}^+ of co-rotating massless particles in the equatorial plane together with the coordinate η_{lr}^- of counter-rotating massless particles and their circumferential radii $R_e(\eta_{\text{lr}}^+)$ and $R_e(\eta_{\text{lr}}^-)$, respectively. Also shown is the location of the ergosurfaces and their respective circumferential radii (solid black).

The general picture is that a single lightring exists, if ω_s exceeds a critical value, which depends on the orientation of the orbit. When ω_s is smaller than this critical value two more lightrings emerge. For the symmetric wormholes one of the lightrings is always located at $\eta = 0$, i.e., at the throat, respectively, at the equator, whereas the remaining ones (if present) are located symmetrically around $\eta = 0$. We note that for symmetric wormhole solutions immersed in rotating ($n = 2$) matter up to five lightrings of counter-rotating massless particles can exist.

When inspecting the circumferential radii for co-rotating and counter-rotating massless particles, which are also exhibited in Fig.5, we realize that the circumferential radius $R_e(\eta_{\text{lr}}^+)$ of the lightrings of co-rotating massless particles and the circumferential radius $R_e(\eta_{\text{th}})$ of the single throat almost coincide for $n = 1$ and are still close for $n = 2$.

We further remark that the ratio E/L of the lightring residing at the equator of the symmetric wormholes becomes negative, when ω_s is smaller than a critical value. The change of sign occurs precisely, when the lightring enters the ergoregion.

IV. CONCLUSION

Whereas previously the rotation of a wormhole spacetime had to be imposed by hand, by requiring a set of non-identical asymptotic boundary conditions for the metric in the two universes [13, 14], we have here obtained a new type of rotating wormhole solutions, which possess identical asymptotic boundary conditions for the metric. Indeed, instead

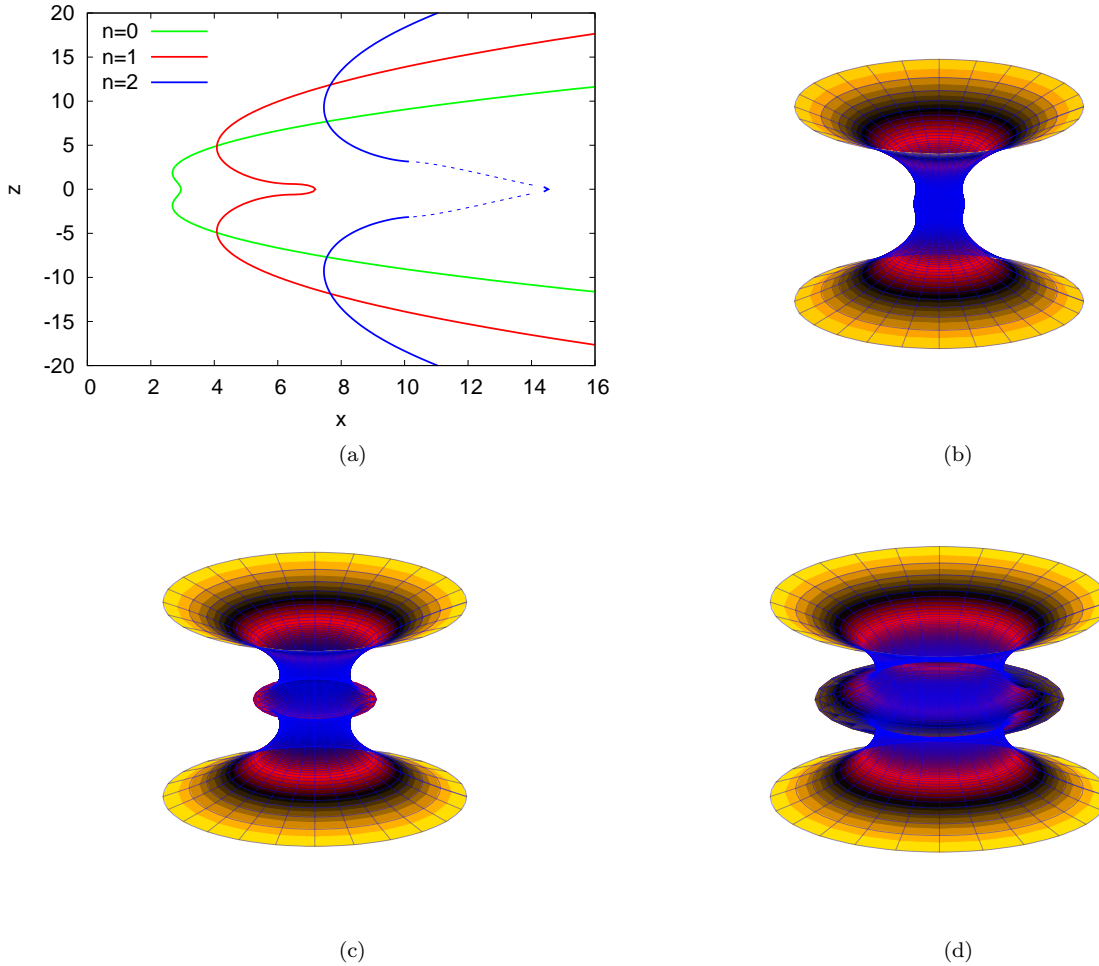


Figure 4: Embeddings of the equatorial plane of symmetric wormhole solutions with throat parameter $\eta_0 = 1$ immersed in non-rotating ($n = 0$) and rotating ($n = 1, 2$) matter: (a) embeddings for $n = 0, 1, 2$ and $\omega_s = 0.3$, where a pseudo-euclidean embedding is indicated by the dashed lines; (b) 3D plot for $n = 0$; (c) 3D plot for $n = 1$; (d) 3D plot for $n = 2$.

of imposing the rotation as a boundary condition we have obtained fully symmetric configurations by immersing the wormholes into rotating matter.

For the rotating matter we have chosen for simplicity a complex massive scalar field without any self-interaction. Both asymptotically flat regions - or universes - possess the same global charges, consisting of the mass, the angular momentum and the particle number, where the latter two are related by the rotational quantum number as in the case of boson stars. We have shown that the resulting configurations can possess interesting physical properties. They can have a single throat or, depending on the parameters, evolve an equator surrounded by a double throat. These rotating wormhole solutions may also exhibit up to five lightrings for counter-rotating massless particles.

The inclusion of a phantom field has allowed for the existence of these topologically non-trivial solutions. Clearly, by replacing General Relativity by certain generalized gravity theories the phantom field would no longer be needed [40–48]. A study of rotating wormholes in such generalized theories would therefore be desirable.

Let us end with a short remark concerning the stability of the above spacetimes. It is known, that the static Ellis wormhole in D dimensions possesses an unstable radial mode [11, 49–51]. Interestingly, when the wormhole throat rotates sufficiently fast, this radial instability disappears, as shown for (cohomogeneity-1) wormholes in five dimensions [12]: As the throat is set into rotation, a non-normalizable zero mode of the Ellis wormhole turns into a second unstable radial mode. With increasing rotation velocity of the throat, the eigenvalue of the original negative mode decreases, while the eigenvalue of the second unstable mode increases, until both merge and disappear. Thus rotation has a stabilizing effect on the wormhole. A stability analysis along these lines for rotating 4-dimensional wormholes represents a challenging future task.

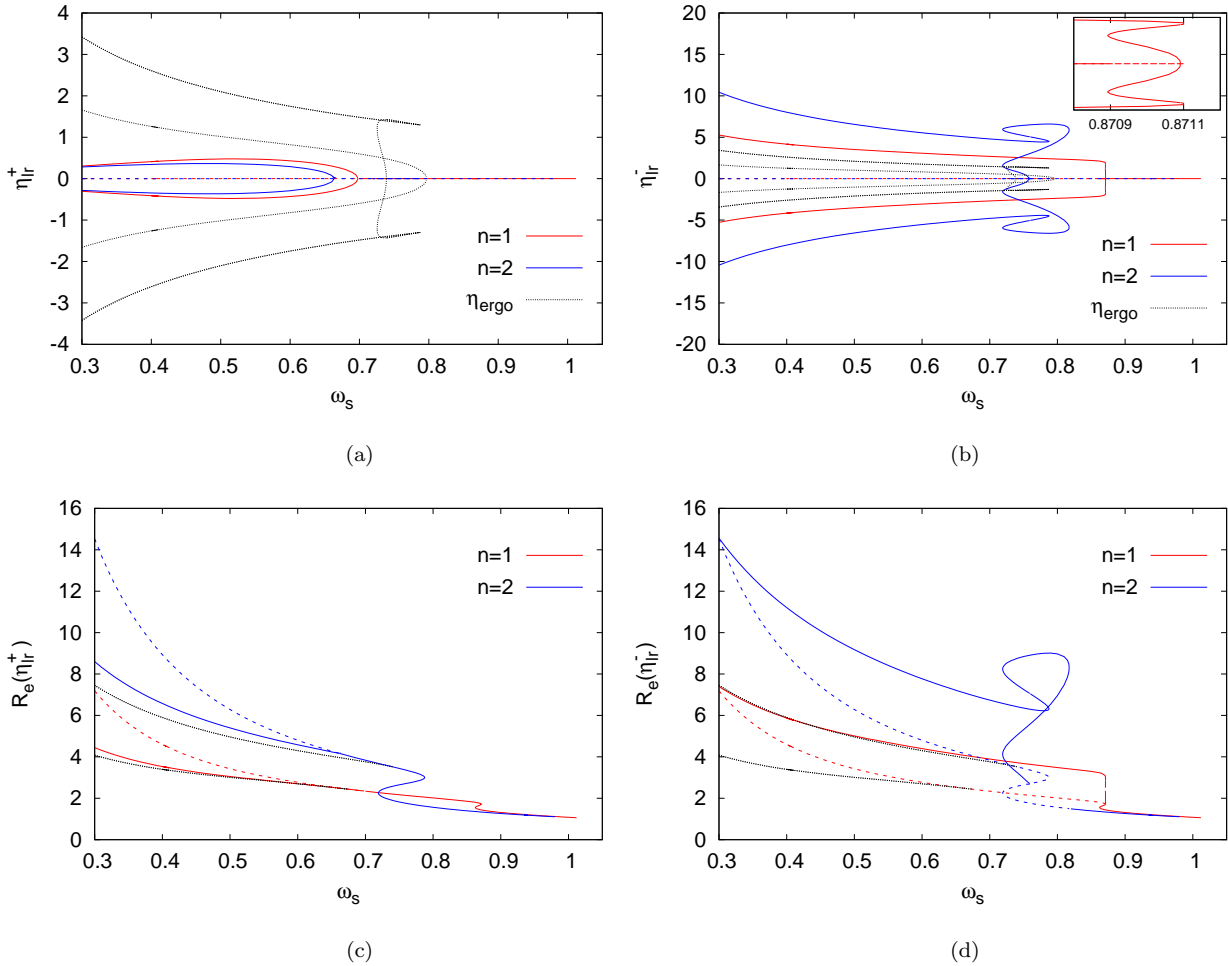


Figure 5: Lightrings of symmetric wormhole solutions with throat parameter $\eta_0 = 1$ immersed in rotating ($n = 1, 2$) matter versus the boson frequency ω_s : (a) the coordinate η_{lr}^+ of co-rotating massless particles in the equatorial plane; (b) the coordinate η_{lr}^- of counter-rotating massless particles in the equatorial plane; (c) the circumferential radius $R_e(\eta_{lr}^+)$; (d) the circumferential radius $R_e(\eta_{lr}^-)$. Also shown are the coordinates and the circumferential radii of the ergosurfaces (black lines).

V. ACKNOWLEDGMENTS

We would like to acknowledge support by the DFG Research Training Group 1620 *Models of Gravity* as well as by FP7, Marie Curie Actions, People, International Research Staff Exchange Scheme (IRSES-606096), COST Action CA16104 *GWverse*. BK gratefully acknowledges support from Fundamental Research in Natural Sciences by the Ministry of Education and Science of Kazakhstan.

-
- [1] H. G. Ellis, J. Math. Phys. **14**, 104 (1973).
 - [2] K. A. Bronnikov, Acta Phys. Polon. **B4**, 251 (1973).
 - [3] T. Kodama, Phys. Rev. **D18**, 3529 (1978).
 - [4] H. G. Ellis, Gen. Rel. Grav. **10**, 105 (1979).
 - [5] M. S. Morris, K. S. Thorne, Am. J. Phys. **56**, 395 (1988).
 - [6] M. S. Morris, K. S. Thorne and U. Yurtsever, Phys. Rev. Lett. **61**, 1446 (1988).
 - [7] C. Armendariz-Picon, Phys. Rev. **D65**, 104010 (2002).
 - [8] S. V. Sushkov, Phys. Rev. D **71**, 043520 (2005).
 - [9] F. S. N. Lobo, Phys. Rev. D **71**, 084011 (2005).
 - [10] F. S. N. Lobo, Fundam. Theor. Phys. **189**, pp. (2017).

- [11] T. Torii and H. a. Shinkai, Phys. Rev. D **88**, 064027 (2013) doi:10.1103/PhysRevD.88.064027 [arXiv:1309.2058 [gr-qc]].
- [12] V. Dzhunushaliev, V. Folomeev, B. Kleihaus, J. Kunz and E. Radu, Phys. Rev. D **88**, 124028 (2013).
- [13] B. Kleihaus and J. Kunz, Phys. Rev. D **90**, 121503 (2014) doi:10.1103/PhysRevD.90.121503 [arXiv:1409.1503 [gr-qc]].
- [14] X. Y. Chew, B. Kleihaus and J. Kunz, Phys. Rev. D **94**, 104031 (2016) doi:10.1103/PhysRevD.94.104031 [arXiv:1608.05253 [gr-qc]].
- [15] B. Kleihaus and J. Kunz, Fundam. Theor. Phys. **189**, 35 (2017).
- [16] F. Abe, Astrophys. J. **725**, 787 (2010) [arXiv:1009.6084 [astro-ph.CO]].
- [17] Y. Toki, T. Kitamura, H. Asada and F. Abe, Astrophys. J. **740**, 121 (2011) [arXiv:1107.5374 [astro-ph.CO]].
- [18] R. Takahashi and H. Asada, Astrophys. J. **768**, L16 (2013) [arXiv:1303.1301 [astro-ph.CO]].
- [19] J. G. Cramer, R. L. Forward, M. S. Morris, M. Visser, G. Benford and G. A. Landis, Phys. Rev. D **51**, 3117 (1995) [astro-ph/9409051].
- [20] V. Perlick, Phys. Rev. D **69**, 064017 (2004) [gr-qc/0307072].
- [21] N. Tsukamoto, T. Harada and K. Yajima, Phys. Rev. D **86**, 104062 (2012) [arXiv:1207.0047 [gr-qc]].
- [22] C. Bambi, Phys. Rev. D **87**, 107501 (2013) [arXiv:1304.5691 [gr-qc]].
- [23] P. G. Nedkova, V. K. Tinchev and S. S. Yazadjiev, Phys. Rev. D **88**, 124019 (2013) [arXiv:1307.7647 [gr-qc]].
- [24] M. Zhou, A. Cardenas-Avendano, C. Bambi, B. Kleihaus and J. Kunz, Phys. Rev. D **94**, 024036 (2016) [arXiv:1603.07448 [gr-qc]].
- [25] V. Dzhunushaliev, V. Folomeev, B. Kleihaus and J. Kunz, Phys. Rev. D **87**, 104036 (2013).
- [26] V. Dzhunushaliev, V. Folomeev, B. Kleihaus and J. Kunz, Phys. Rev. D **89**, 084018 (2014).
- [27] A. Aringazin, V. Dzhunushaliev, V. Folomeev, B. Kleihaus and J. Kunz, JCAP **1504**, 005 (2015) doi:10.1088/1475-7516/2015/04/005 [arXiv:1412.3194 [gr-qc]].
- [28] E. Charalampidis, T. Ioannidou, B. Kleihaus and J. Kunz, Phys. Rev. D **87**, 084069 (2013) doi:10.1103/PhysRevD.87.084069 [arXiv:1302.5560 [gr-qc]].
- [29] V. Dzhunushaliev, V. Folomeev, C. Hoffmann, B. Kleihaus and J. Kunz, Phys. Rev. D **90**, 124038 (2014) doi:10.1103/PhysRevD.90.124038 [arXiv:1409.6978 [gr-qc]].
- [30] C. Hoffmann, T. Ioannidou, S. Kahlen, B. Kleihaus and J. Kunz, Phys. Rev. D **95**, 084010 (2017) doi:10.1103/PhysRevD.95.084010 [arXiv:1703.03344 [gr-qc]].
- [31] F. E. Schunck and E. W. Mielke, in *Relativity and Scientific Computing: Computer Algebra, Numerics, Visualization*, eds. F. W. Hehl, R. A. Puntigam, and H. Ruder, (Springer Berlin Heidelberg, 1996)
- [32] W. Schönauer and R. Weiß, J. Comput. Appl. Math. **27**, 279 (1989) 279; M. Schauder, R. Weiß and W. Schönauer, *The CADSOL Program Package*, Universität Karlsruhe, Interner Bericht Nr. 46/92 (1992).
- [33] P. Jetzer, Phys. Rept. **220**, 163 (1992).
- [34] T. D. Lee, Y. Pang, Phys. Rept. **221**, 251 (1992).
- [35] F. E. Schunck, E. W. Mielke, Class. Quant. Grav. **20**, R301 (2003).
- [36] S. L. Liebling and C. Palenzuela, Living Rev. Rel. **15**, 6 (2012) doi:10.12942/lrr-2012-6
- [37] B. Kleihaus, J. Kunz and M. List, Phys. Rev. D **72**, 064002 (2005).
- [38] B. Kleihaus, J. Kunz, M. List and I. Schaffer, Phys. Rev. D **77**, 064025 (2008).
- [39] B. Hartmann, J. Riedel and R. Suci, Phys. Lett. B **726**, 906 (2013).
- [40] D. Hochberg, Phys. Lett. **B251**, 349 (1990).
- [41] H. Fukutaka, K. Tanaka, K. Ghoroku, Phys. Lett. **B222**, 191 (1989).
- [42] K. Ghoroku, T. Soma, Phys. Rev. **D46**, 1507 (1992).
- [43] N. Furey, A. DeBenedictis, Class. Quant. Grav. **22**, 313 (2005).
- [44] K. A. Bronnikov and E. Elizalde, Phys. Rev. D **81**, 044032 (2010).
- [45] P. Kanti, B. Kleihaus and J. Kunz, Phys. Rev. Lett. **107**, 271101 (2011).
- [46] P. Kanti, B. Kleihaus and J. Kunz, Phys. Rev. D **85**, 044007 (2012).
- [47] F. S. N. Lobo and M. A. Oliveira, Phys. Rev. D **80**, 104012 (2009).
- [48] T. Harko, F. S. N. Lobo, M. K. Mak and S. V. Sushkov, Phys. Rev. D **87**, 067504 (2013).
- [49] H. -a. Shinkai and S. A. Hayward, Phys. Rev. D **66**, 044005 (2002).
- [50] J. A. Gonzalez, F. S. Guzman, and O. Sarbach, Class. Quant. Grav. **26**, 015011 (2009).
- [51] J. A. Gonzalez, F. S. Guzman, and O. Sarbach, Class. Quant. Grav. **26**, 015010 (2009).